An Anthropological and Paleopatological Research of Human Skeletons from Buries 7c. BC from Nor Armavir Burial Ground (Armenia)*

• Anahit Yu. Khudaverdyan, Simon G. Hmayakyan, Nvart G. Tiratsyan, Margar S. Hmayakyan •

Institute of Archaeology and Ethnography, National Academy of Science, Republic of Armenia

Address for correspondence:

Anahit Yu. Khudaverdyan
Institute of Archaeology and Ethnography,
National Academy of Science,
Republic of Armenia
E- mail: akhudaverdyan@mail.ru

Bull Int Assoc Paleodont. 2020;14(1):53-78.

Abstract

The material of the study was the skeletal remains of 10 individuals (one man, three women, 5 children and one individual without sex definition) discovered in August 2019 during excavations of New Armavir grave. For the first time, a comprehensive paleoanthropological analysis of the data was obtained for this grave. The study was carried out by visual examination of skeletons and radiography. Traces of pathological processes on skeletons have been revealed and their etiology has been reconstructed. The structure of the paleopathological profile of the sample is dominated by inflammatory diseases, abnormalities and injuries. The tradition of inadvertently changing the shape of the head in a given sample probably caused a specific way of caring for the infant in the early years of his life and a long stay in a certain cradle. Two craniological complexes can be conditionally isolated as part of this group. The first is of the low-head mesocrane type, the second high-head dolichocrane type. The odontological complex is of the southern graceful type with a high level of reduction of the hypoconus of the second upper molars, small tooth sizes. At the individual level, the total size and shape of the body of the adult population has been analysed. Labour burdens are recorded in both women and men. It has been established that the state of health of individuals buried in the grave was unsatisfactory, as evidenced by the large number of pathologies. In our study, 5 out of 4 children skeletons with evident lesions, that were defined as diagnostic of scurvy. An anthropological analysis of 10 skeletons revealed at the 4 individuals penetrating wounds on the skeletons. Although considerable uncertainty remains, we believe that the most likely conclusion is that Nor Armavir burials represent a place for at least some sacrificed individuals dedicated as offerings.

Keywords: Armenia; Urartu; physical anthropology; human osteology; odontology; paleopathology; roentgenology

** Authors are responsible for language correctness and content.*

Introduction

Armavir is one of the ancient capitals of Armenia that was a large commercial city located 1 km west village of Armavir. The area of ancient Armavir was inhabited since the 4 - 3th millennium BC. Armavir was regarded as an ancient capital of Armenia, said according to legend to have been founded by King Aramais in 1980 BC (1). The city was first described by Movses Khorenatsi (Moses of Khoren) in the 5th-century CE (1). During the first half of the 8th century BC, King Argishti I of Urartu built a fortress in the area and named it Argishtikhinili. On the territory of the city, 21 cuneiform inscriptions on stone were found (some of which were published by the monks of Etchmiadzin), three clay plates with wedge-shaped inscriptions in Elam language. Rock inscriptions in ancient Greek were also found, with excerpts from the works by ancient Greek authors. Both hills (Armavir and the “fortress /hill of St. David”) are still a place of religious worship. The Armavir archaeological expedition was led by N.Ya. Marr, S.V. Ter-Avetisyan, S. Ter-Hakobyan, B.N. Arakelyan, A.A. Martirosyan, R.M. Torosyan, G.A. Tiratsyan, I.A. Karapetyan, S.G. Hmayakyan.

This article considers the bioarchaeological analysis of the 10 skeletal individuals that were unearthed from the seventh-century BC in Nor Armavir cemetery (Armenia), during excavatins in 2019 (Figure 1). The village of Nor Armavir is located in the northwest of the "fortress of St. David." Here, in all, 24 burials of the 8th-6th centuries BC were discovered and excavated of which 15 in karas (large ceramic vessels: Pythos) (2).

Materials and methods

The human remains that were analyzed and that are discussed herein were excavated in the 2019 by a team of archaeologists (Simon G. Hmayakyan, Nvart G. Tiratsyan, Margar S. Hmayakyan) from Institute of Archaeology and Ethnography, National Academy of Science of Armenia under the direction of Simon G. Hmayakyan at the Nor Armavir site (Figure 1). During excavations, a red karas burial of one individual (No. 7) was found, with rich inventory (Figure 1b). Nearby stood a second karas, fragmented and empty. The material of the study was the skeletal remains of 10 individuals (men, three women, 5 children and one without sex definition). The material is kept at the Laboratory of physical anthropology of the Institute of Archaeology and Ethnography, NAS RA in Yerevan.To record the determination of age at death, sex, stature, pathological and dental analysis, completeness and preservation (Figure 2) of the human remains, standardized forms were used. Sex assessment of males and females was accomplished by observing morphological traits on both the skull and the os coxae or pelvis, according to Acsádi and Neméskeri (3) and Buikstra and Ubelaker (4), and by giving priority to the pelvis (5). Assessment of age was undertaken by using the following methods: the symphyseal phase of the pubic symphysis, the stage of the auricular surface, the sternal ends of ribs and the obliteration stage of the endocranial and ectocranial sutures, and the occlusal surfaces of all dental elements (3, 4, 5, 6, 7, 8, 9). The age of subadults was assessed on the basis of the changes that occur during the development and formation of deciduous and permanent teeth, the degree of bone ossification, and the length of the diaphysis of long bones (Atlas of human tooth development and eruption: 10).

Next, a series of standard measurements are taken of the skulls, bones and teeth, and the presence and absence of “non-metric traits” (11, 12, 13). Measurements were taken as outlined in Alexseev (14). The results are shown in Table 1. Maximum bucco-lingual and maximum mesiodistal diameters were measured for each tooth in the dental arcade, following Zubov (12, 13). Non-metric dental traits definitions and code matching for the ranked traits used in the study (Zubov scheme) and in the Arizona State University Dental System (ASU scheme) cited according to Haeussler and Turner (15) and Khudaverdyan (16). The study of non-metric characteristics is mainly focused on describing differences and similarities between populations, or on the affiliation between individuals within one group (16). It is also suggested that some non-metric traits such as squatting facets may be related to occupational behaviour (17).

The bone is measured on an osteometric board, and stature is then calculated using a regression formula developed upon individuals of known stature (18, 19). The average adult stature was measured by the following three methods: the measurements of the present complete long bones of the lower and upper extremities, followed by the application of the tables by Trotter

Figure 1 Nor Armavir burial ground, excavations 2019, sanctuary over burials (a), jugs and in situ materials (b), jug (c).

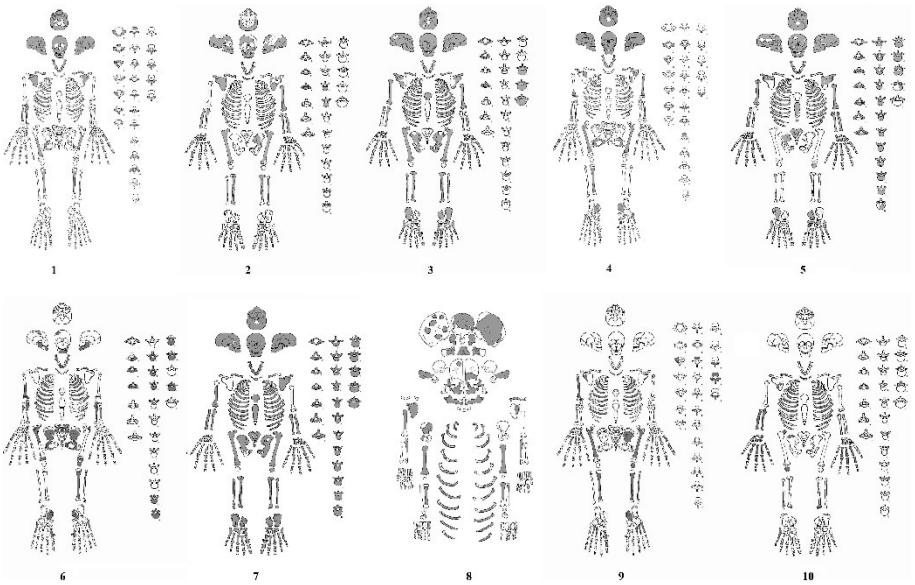

Figure 2 Skeletal inventory from the Nor Armavir burial ground.

Figure 3 Individual No 1.

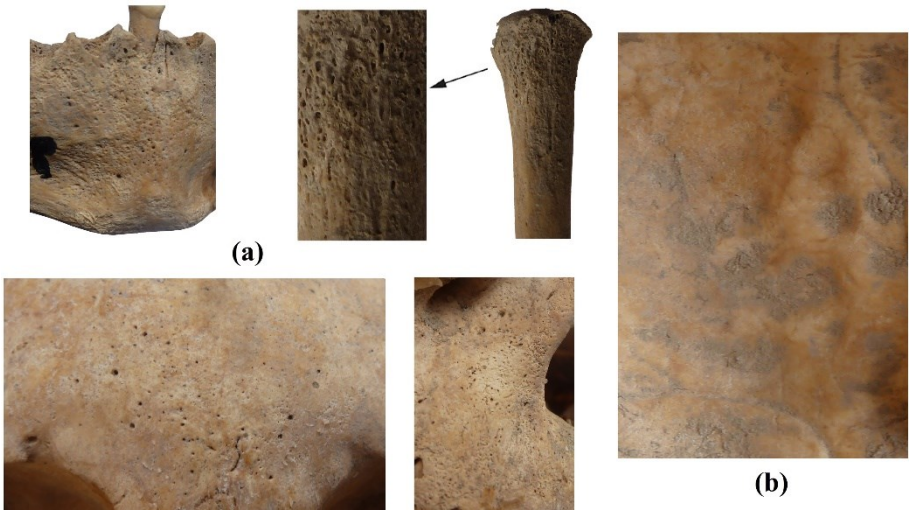

Figure 4 The cribra cranii externa, porotic bone, the endocranial surface of the cranial vault fragment, showing the convolutional markings in the central part.

(18) for males, and Trotter and Gleser (19) for females. The activity marker registration was based upon a macroscopic analysis of the skeletal elements under study.

In addition, the skull and the postcranial skeleton were examined macroscopically and X-ray to investigate any pathological changes. To record pathological lesions on the skeleton, a classification of diseases and injuries was formulated according their aetiology, and consists of the following diseases: joint disease, trauma, infectious disease, metabolic disease, neoplastic disease, etc. (17). Further, other anomalies and observed enthesopathies have been recorded. When a muscle joint endures a severe repetitive pattern of stress, it is suggested

that this is caused by a specific occupation or activity. Situated at tendon and ligament insertions they might imply an intense use of certain muscles when new bone formation at the site of a muscle attachment occurs (17).

Results

Ten skeletal individuals have been analysed from which 1 have been determined as male, 3 as female adults, 5 children, one individual without sex definition).

Individual No 1.

The individual was identified as an infant aged 4-6 years. The complete cranium is in a fairly good state of preservation (Figure 2). Of the 20 deciduous teeth, only 11 were found in the alveolus and the first permanent molar. The cranial index was 70.8, which placed it in the dolikhocran range, the upper facial index indicates a broad face (eurien), orbits high, nose wide (Table 1). Of the 39 cranial nonmetric traits only fourteen were found (foramina supraorbitalia, foramina zygomaticofacialia, os zygomaticum bipartitum, spina processus frontalis ossis zugomatici (direct), Os wormii suturae sagittalis, foramina parietalia, os wormii suturae lambdoidea, foramina mastoidea (out of the seam), sutura palatina transversa (Π-shaped), sutura incisive, canalis craniopharyngeus, canalis condyloideus, sutura mendoza) (Table 2). Teeth of the individual are characterised by Carabelli cusp on the upper first molar M1 (score 4), 1 pa (3) UM1: type 3 of the first paracone (eocone) groove on the upper first molar, oblique ridge on the upper first molar, tuberculum accessorium mediale internum or tami, deflected metaconid wrinkle on the lower first molar and the variant 2med II position of the second furrow of the lower first molar metaconid. The external surface of the skull shows flat, porous. The alteration is most remarkable on the glabella, the orbital regions of the frontal, the sphenoid and the maxillae all show bilateral and symmetrical fine porotic (Figure 4a). Porous lesions are also apparent on the anterior surfaces of the maxillae surrounding the infraorbital foramina, below the anterior nasal spine. Fine porotic new bone formations are visible at various locations on the mandibular body. The postcranial skeleton is also affected. Each preserved long bone exhibits fine porous lesions. On the basis of the macromorphological characteristics of the observed lesions, the most likely diagnosis was scurvy. The child has, an early stage of this disease was supposed. Child abuse, such as “shaken baby syndrome” or other forms of abuse, might cause bleeding all over the body, including subperiosteal haemorrhages. However, bilaterally symmetrical appearance of the alterations is uncommon, and therefore the possibility of this aetiology is very low (20, 21). Considering the macromorphological features of the lesions, the distribution pattern of the changes and their comparison with the features of the other possible aetiologies (e.g. infectious conditions, such as sinusitis frontalis, non-specific periostitis and osteomyelitis or tuberculosis, rickets, anaemia), we can establish the diagnosis of scurvy.

It is necessary to dwell at upon on one more traits (digital impressions). Digital impressions, also known as convolutional markings, on the inner surface of the skull (Figure 4b) (i.e., shallow depressions resembling to the imprint of a finger and corresponding to cerebral gyri that are intervened by thicker bony ridges corresponding to cerebral sulci) are probably formed by localised pressure of the pulsating brain underlying the bone. Pronounced digital impressions, generally confined to the base and lower two-thirds of the skull vault, may be normal in childhood (particularly during periods of rapid brain growth), their prominence decreases during adolescence.

Individual No 2.

Sex determination and age at death estimation, carried out on the basis of several highly diagnostic features; identify the individual as a young adult. Results of metric and morphologic analyses of the pelvis concur in indicating female sex. Age-at-death estimates, obtained using various parameters – cranial sutures synostosis, pubic symphysis morphology, ilium auricular surface morphology, are all in agreement with an age 29 years. The maximum cranial breadth is medium wide, the cranial base lengths is in the range of very large values. The occipital breadth is medium. Of the 25 cranial nonmetric traits only six were found (foramina zygomaticofacialia, processus temporalis ossis frontalis, os wormii suturae squamosum, foramina parietalia, os wormii suturae lambdoidea, sutura incisiva).

Sizes of teeth measurements the individual are listed in Table 2. Protostylid was noted on the right mandibular third molar (Figure 5). Protostylid on the molar was located on hypoconid (distobuccal cusp), and extended till the occlusal surface of the tooth (ASUDAS 3–7). It was conical in shape with its base blending with the cervical portion of the buccal surface and a

flat free cusp apex. This cusp was separated from the tooth by deep developmental grooves. Teeth of the individual are characterised also by tuberculum accessorium mediale internum or tami, deflected metaconid wrinkle on the lower third molar and the distal trigonid crest on the lower third molar.

Figure 5 Protostylid in the lower right third molar.

Basic of limb bone measurements the individual are listed in Table 3. The maximal length left humerus is small, the minimal diaphysis circumference is characterized as small. Robusticity index - medium. The physiological length of the right radius is of medium. The individual was with a mean of 152.4cm. Strong tuberosities of m. deltoideus, distinctive tuberositas radii. Femurs show strong tuberositas glutaea, trochanter tertius forms a bony protuberance, strongly developed attachment sites for the knee extensors.

Analysis revealed the presence of cranial trauma to individual. There appears to have been blunt force trauma to the frontal bone (Figure 6a) and circular lesion (perimortem) that were caused by a weapon with a blunt, circular striking surface (Figure 6b). The evidence for trauma in archaeological populations is restricted to that visible in the skeletal remains, unless soft tissue is preserved (17). Evidence of violence is most often seen on the skull; it is assumed that such blows are meant to be fatal. Antemortem injuries occurred during life and show evidence for healing, whereas peri-mortem injuries occurred around the time of death and consequently no evidence for healing will be seen. Generally, postmortem breaks will have a paler surface than the surrounding bone and broken edges will usually be perpendicular to the bone (22), whereas fractures that occurred around the time of death will be stained the same color as the surrounding bone (17).

A small dental chipping (1.5 mm) with smooth edges on the cutting edge, was detected on the upper incisors. The appearance of the chip might be accounted for by the necessity of biting off threads.

Individual No 3.

Individual 3 is an aged adult male, 60+ years old. All teeth were lost antemortem. The skull of the individual is characterized as dolikhocranic, the occiput and forehead is of wide (Table 1). The zygomatic diameter is medium. Both the nasal height and the nasal breadth are middling. The tuberosity on the external surface of the angle (the reposition of the mastication muscle, m. masseter) and the internal surface of the angle (the reposition of the internal wing muscle m. pterygoideusmedialis) is distinctly discerned on both sides. Twenty-one of the forty-four studied discrete-varying markers are found in individual (spina trochlearis, foramina zygomaticofacialia, os zygomaticum bipartitum, spina processus frontalis ossis zugomatici /protrusion/, stenocrotaphia /X-shaped/, processus frontalis squamae temporalis, processus temporalis ossis frontalis, os wormii suturae squamosum, os postsquamosum, foramina parietalia, os asterion, foramina mastoidea, sutura palatina transversa (П-shaped), canalis craniopharyngeus, отсутствие foramina spinosum, tuberculum praecondylare, foramina mentalia).

According to the absolute dimensions, the brachial bone is characterizedby the medium values. The supracondylar process (processusepi condyloides) of the left brachial bone is fixed on the inner crest of the body above the medial condyle. The structure of the upper part of the diaphysis of the ulna is normal; the section does not have a specialized form - eurolining. The length of the femurs and tibias also medium. There is an additional articular area on the lower articular surface of the tibia. The present individual had a height of approximately 165 cm (Table 3).

Traces of physical exertion are observed on the bones of the upper and lower limbs (Table 4). The crest of the lesser tubercle, the intertubercular sulcus of the humerus and the deltoid tuberosity of the humerus are fairly well developed on the humeral bones. On these grounds, the average values are totally equal to 2.63. Suchlike development of the deltoid tuberosity of the humerus testifies to the strong development of the muscle of the same name which raises the upper limb up to a horizontal level and rotates the

Figure 6 Frontal bone injuries.

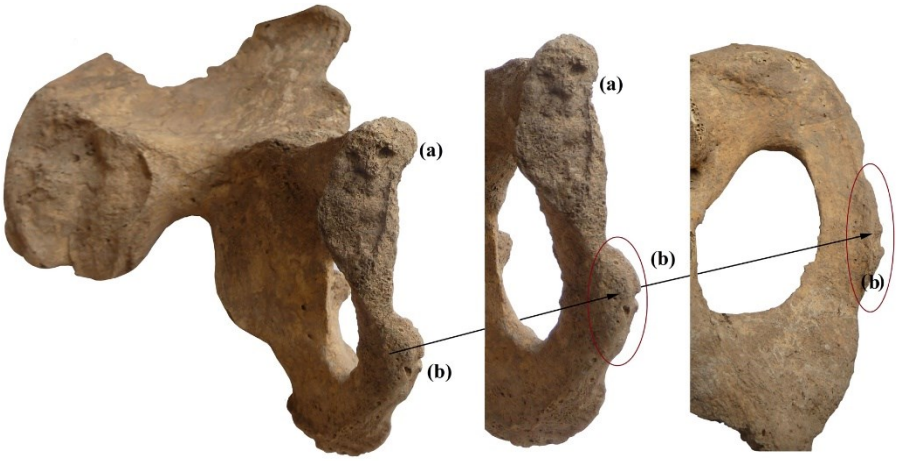

Figure 7 Pubic symphysitis (a), ischiopubic ramus injury (b).

shoulder inward and outward which in its turn suggests a developed muscular shoulder. On the whole, we can talk about the great significance of the working activities of the individual's muscles which raise and rotate the shoulder. The quadrate pronator muscle is attached to the distal-lateral crest that is well developed on ulnar bones.

Traces of considerable functional load are fixed on the symphysis, on the pelvic bones. Traces of enthesopathy were formed at the attachment points of the superior pubic ligament (ligamentum pubicum superious) and the arcuate ligament of pubis (ligamentum arcuatum pubis). Bone lysis sectors are seen in the form of round holes with a diameter of 1-2 mm on the articular surfaces of the pubic bones (simphysispubica) (Figure 7).The reason for their appearance may be the pubic symphysitis which is part of the multicomponent ARS-syndrome (adductor, rectus, symphis) - a pathological condition of the tendon muscle complex that developed as a result of prolonged and similar loads associated with the asymmetric adductor brevis muscle of the thigh (musculus adductor longus et (or) brevis) and the distal part of the abdominis rectus muscle (musculus rectus abdomonis).The gait, requiring the body to tilt forward when fixing the tibia in a straight or bent position, may lead to trauma.

Trauma can result from acute events both from accidents and interpersonal violence, or it can be the result of chronic stress associated with work or daily activity. Fractures to the pelvis usually result from a force that is transmitted longitudinally through the femur resulting from direct injury or violence (22, 23). The most common of this variety is a fracture of the inferior ischio-pubic ramus (Figure 7b). The mechanism of injury can be an anterior-posterior crushing force, compression from side to side, or a vertical shearing force (22, 23). Teh et al. (24) found that

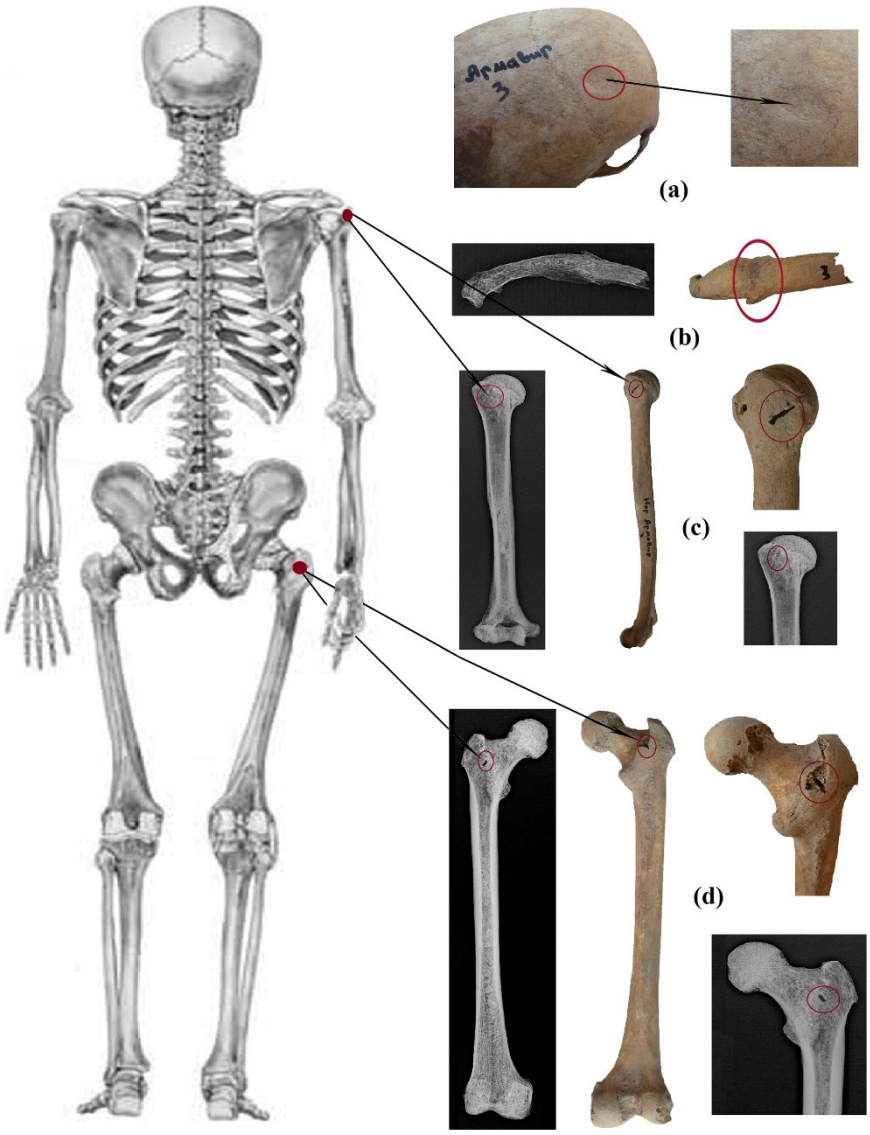

Figure 8 Antemortem and perimortem injuries.

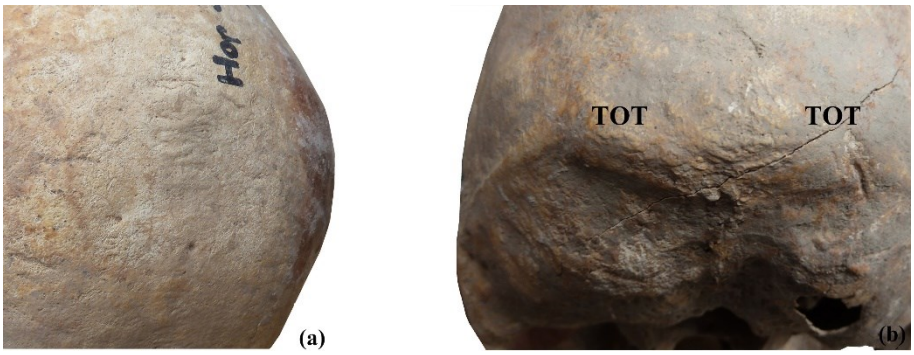

Figure 9 Unintentional deformation (cradle deformation) (a), occipital superstruct (torus, TOT) (b).

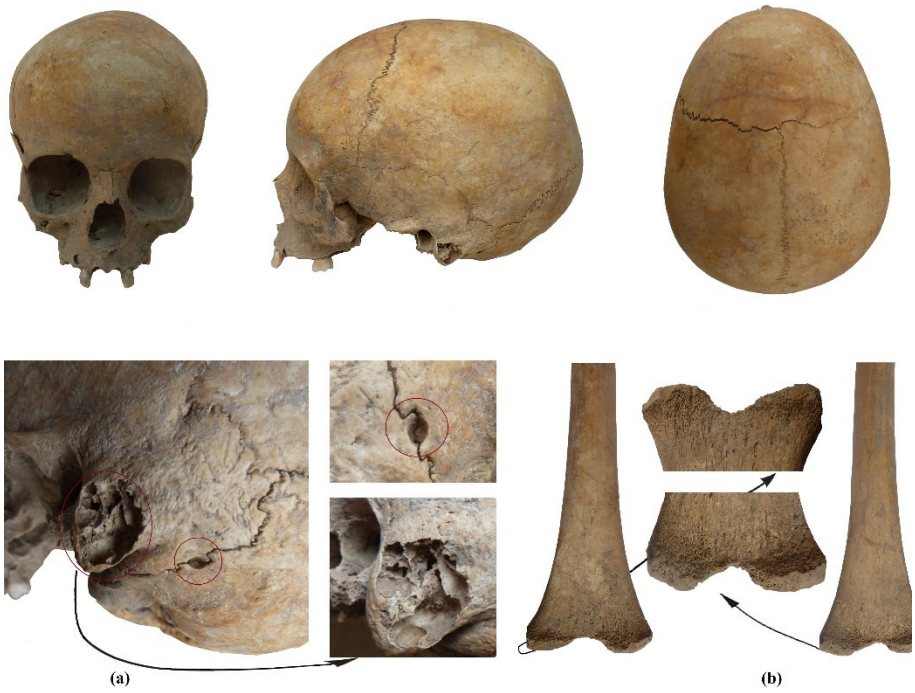

Figure 10 Otitis media, cloaca in the left occipital-mastoid suture, porous in the lower femoral epiphyses.

Figure 11 Septal aperture.

fractures in this area were due mostly to forces transmitted from the femur, which passed through the hip joint.

Poirer's facets located on the superolateral third of the femur at individual. This type of bone-changing stress is caused by habitual hip extension and stabilization with an upright posture necessary to maintain balance (25). To do this, the gluteus maximus muscles must be extended for stability (25). These are found

among modern athletes including - football players, skiers, and horseback riders‖ (25). Due to the physical strain necessary to create these enthesopathies in an ancient population, horseback riding or constant traversing of mountainous terrain would be probable causes (26). Individual has the bilateral enthesopathies on the superiolateral third of the femoral diaphysis inferior to the lesser trochanter and lateral to the linea aspera. This is the insertion area for the gluteus maximus muscles (25). Stress traumas are caused by habitual physical activity. Given the location of these enthesopathies, it can be suggested that individual was habitually sitting, thighs apart, on a surface that required stability maintenance. The posterior surface of tibia corresponding to the soleal line of tibia (the third head of triceps muscle of calf) is moderately (not weakly) developed.The relief on the posterior surface of both tibias corresponding to the soleus line (third head of the triceps tibia muscle) is very good developed.

Individual 3 shows cranial pathology that may indicate active healing of past injurie. There are depressions on the frontal bone and is oval in shape with a length of 22mm and a height of 10mm (Figure 8a). Is observed traumatic sixth rib fracture. Fracture occurs near the angle (see Figure 8b). Fractures of the ribs can have varied causes, which range from direct injury, to falls against hard objects, habitual labor, violent coughing, and in some cases laughing (22,23). For example, a force that originates from the front will produce a fracture near the angle, whereas a force from the back will cause a fracture closer to the spine. In cases where a force is applied from the sides, there is the potential for both the area near the spine and the sternum to be affected (22). The fifth through ninth ribs are most often fractured, with the right side favored in a majority of cases. Teh et al. (24) found that individuals who jump from a height have more right rib fractures on average, in contrast to fallers who have about equal rates of rib fracture for each side.

The proof for perimortem trauma on that individual is demonstrated in Figure 8c and d. The right humerus demonstrated one chop stab across of lesser tuberosity and this trauma measured 16mm in length (Figure 8c). The second bone with features of perimortem trauma was the right femur, which had one chop mark (punch blade) located on the intertrochanteric crest, which measured 17mm in length (Figure 8d). The blade had fully pierced the bone and left distinct entry (Figure 8d). All of the chop marks on this individual were very much straight. The number of skeletal fractures (3 antemortem and 2 perimortem) emphasises the fact that for this male from Nor Armavir, interpersonal violence was an ever-present aspect of life. Acute power trauma results from assault with a bladed weapon, such as a sword. We suppose that he had died in battle. Warfare (and raiding as part of it) is a probable interpretation for this violence.

Figure 9 shows several modifications that are recognizable on the vault: amarked depression immediately above the lambda affecting the mid-sagittalcontour, resulting in an interparietal plane which covers nearly half of the sagittalsuture. The flattenedarea is roughly circular with bilateral dimensions roughlyequal (Figure 9a). The flattened surface thus slopes to the top above the lambda. This flattening is a deformation that could have been effected by the infantlying on the back with the head resting on the occiput. Thus, cradle deformationis heavily influenced by infant sleep position, and constant supine positioning is afrequent cause of deformation during infancy (27). Tubercle development on the occipital torus (TOT), at the trapezius (m. trapezius occipitalis) attachment site, represents a secondary superstructural development on top of a superstructure (28) (Figure 9b). The degree of expression of TOT is estimated for individual is it well developed (score=3).

Individual No 4.

The skeleton belongs to a child of 8-10 years (Figure 10). The skull is characterized as mezocranic, the nasal breadth are medium, orbits medium (Table 1). Fourteen of the forty-three studied discrete-varying markers are found in individual (foramina zygomaticofacialia, spina processus frontalis ossis zugomatici /straight/, stenocrotaphia /X-shaped/ processus temporalis ossis frontalis, os wormii suturae squamosum, foramina parietalia, os wormii suturae lambdoidea, foramina mastoidea, sutura palatina transversa /П-shaped/, sutura incisive, condylus occipitalis bipartitum, canalis condyloideus, sutura mendoza). Both the mesio-distal and vestibule-lingual (Table 2) sizes of the molars fall into the category of vary very small, small and medium. On the second molars, the hypocone is strongly reduced (score 3+), and the metaconus is markedly reduced.

Pathological changes were detected in the individual. Otitis media is the infection of the inner ear which is detected in child. Inflammation of the pharynx causes swelling within the ear which

creates a stagnant pool of fluid that is perfect for bacterial growth. Eventually the fluid has to escape and this is seen on the surface of the left-t occipital-mastoid suture. The infection has produced a smooth walled cloaca with the appearance of an accessory foramen that passes through the masto-occipital suture (Figure 10). The bacteria eat away lytic-looking areas of bone. For an individual that constantly suffers this type of infection, the bacteria may spread into the cranial cavity infecting meningeal arteries and other areas of blood supply which could lead to gradual septicemia (29).
All spongy bone, including that of the vertebral bodies, is porous.

Individual No 5.
The skeletal remains is belongs to a 50-59 year-old female (Figure 3). The skull relief is poorly developed. The skull of individual is also mezocranic, the forehead is wide, and the occiput is of medium. The degree of expression of TOT is estimated for individual is medium developed (score=2). The face height is medium, the nasal height is large, nasal breadth are medium (Table 1). The orbits are of medium height and wide. The projection length of the lower jaw is medium. Sixteen of the forty-seven studied discrete-varying markers are found at the skull (foramina zygomaticofacialia, os zygomaticum bipartitum, spina processus frontalis ossis zugomatici (outgrowth), stenocrotaphia /X-shaped/, processus temporalis ossis frontalis, os wormii suturae squamosum, foramina parietalia, foramina mastoidea, torus palatines (point 1), sutura palatina transversa /П-shaped/, sutura incisive, canalis craniopharyngeus, tuberculum praecondylare, foramina mentalia).
The occlusal surface of the left lateral incisor and first upper premolar have a Scott (30) wear score of 36 indicating attrition into the dentin and the presence of only a thin rim of enamel on all four quadrants, although some was broken off postmortem. Dental wear of the functional chewing surface depends on the hardness of food consumed and on whether the teeth are used as tools. Only left lower canine examined.The marginal ridges of the lingual surface were slightly expressed in the canine. The mesio-distal size = 6.2mm, vestibule-lingual = 7,8mm. Dental calculus is fixed on the canine; also a weak form of the linear enamel hypoplasia was detected. The formation of dental calculus has a complex etiology and to a large extent depends on the nature of the consumed food. Enamel hypoplasias are the result of physiological stress induced disruptions in amelogenesis which produces visible defects in the dental enamel that typically manifests as either horizontal lines on the anterior portion of the tooth (31, 17).
Individual 5 also has evidence of five buccal maxillary periapical lesion (also known as ‘abscesses’). Above the right maxillary molars is an irregular area with pitting on the internal and external surfaces, complete resorption of the posterior alveolus and active resorption of the anterior alveolus, indicating the spread of infection from the dentition into the maxilla above the alveolus. Lost teeth are recorded as lost ante mortem when there is no alveolus present, or when the alveolus is partly resorbed. When the alveolus shows no signs of resorbtion the tooth is recorded as lost post mortem. The individual lost first lower molar antemortem.
According to the absolute dimensions, the brachial bone is characterizedby the medium size, minimal shaft circumference of small values (Table 3). The supracondylar process (processus epicondyloides) of the right brachial bone is fixed on the inner crest of the body above the medial condyle (Figure 12). An individual also shows areas of resorption in the area of the diaphysis humerus (Figure 12). The ulna and radius are also in all dimensions characterized by medium values. The present individual had a height of approximately 159 cm. Traces of physical exertion are observed on the bones of the upper limbs (Table 4). The crest of the lesser tubercle, the intertubercular sulcus of the humerus and the deltoid tuberosity of the humerus are fairly well developed on the humeral bones. Traces of considerable functional load are fixed on the symphysis, on the pelvic bones. Traces of enthesopathy were formed at the attachment points of the superior pubic ligament and the arcuate ligament of pubis. Bone lysis sectors are seen in the form of round holes with a diameter of 1-2 mm on the articular surfaces of the pubic bones (simphysis pubica).The reason for their appearance may be the pubic symphysitis.
The synostosis of the 2th and 3th cervical vertebrae is present (Figure 13a). The complete union occurred between the articular facets, total fusion between the posterior elements was also detected. The lateral direction roentgenogram reveals that the fusion of the posterior parts are complete, the radiolucent areas between the two

Figure 12 Septal aperture, resorption in the area of the diaphysis and pineal gland.

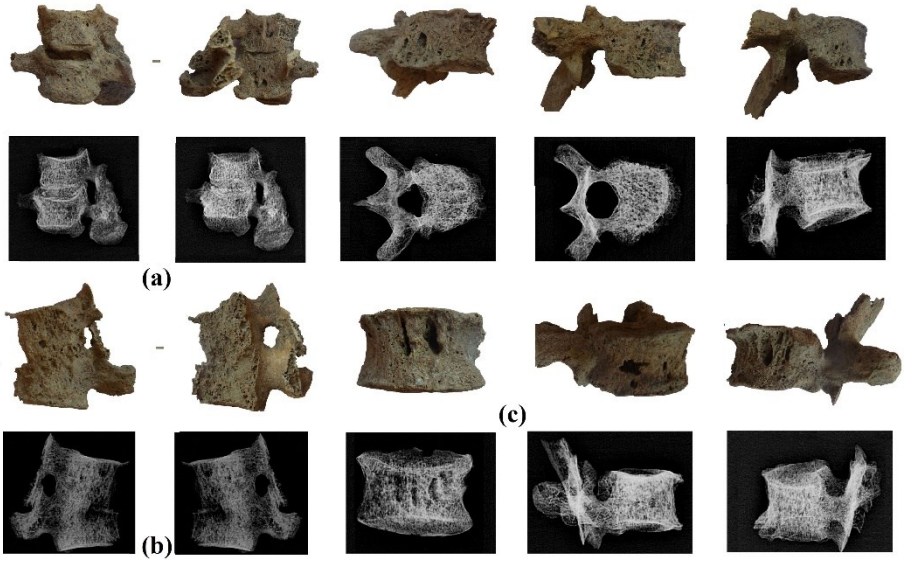

Figure 13 Cervical (a) and thoracic ankylosis (b), tuberculous foci and degenerative changes of the vertebrae (v).

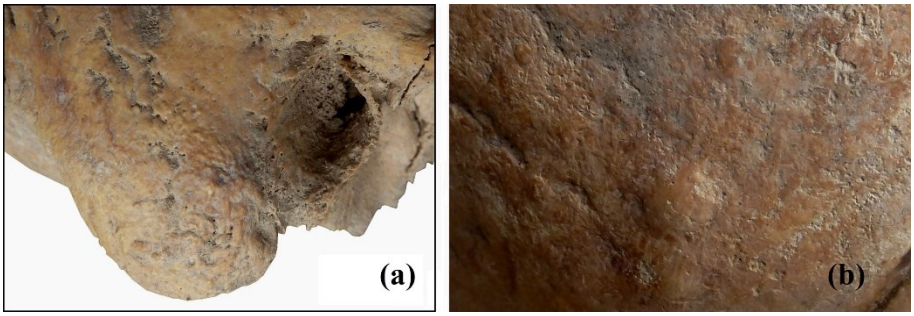

Figure 14 Exostoses of the internal auditory canal (a) and osteoma (b) on the right parietal bone.

Figure 15 Perimortem injuries of the left innominate bone and 1st lumbar vertebra.

Figure 16 Pythos burial, individual No 7.

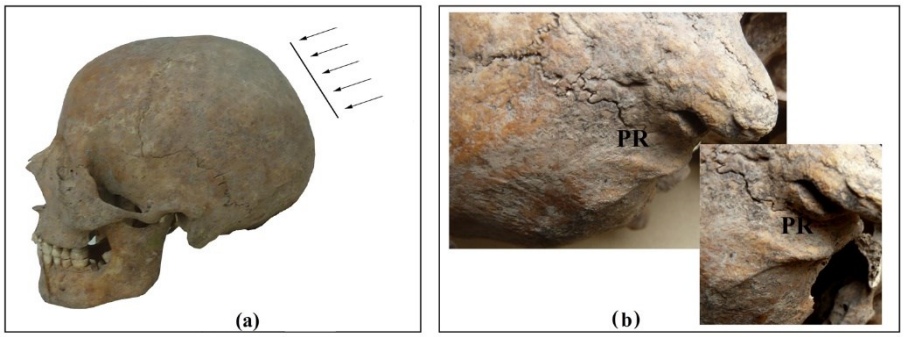

Figure 17 Unintentional artificial deformation of the parieto-occipital region, retromastoid process (PR, score 2).

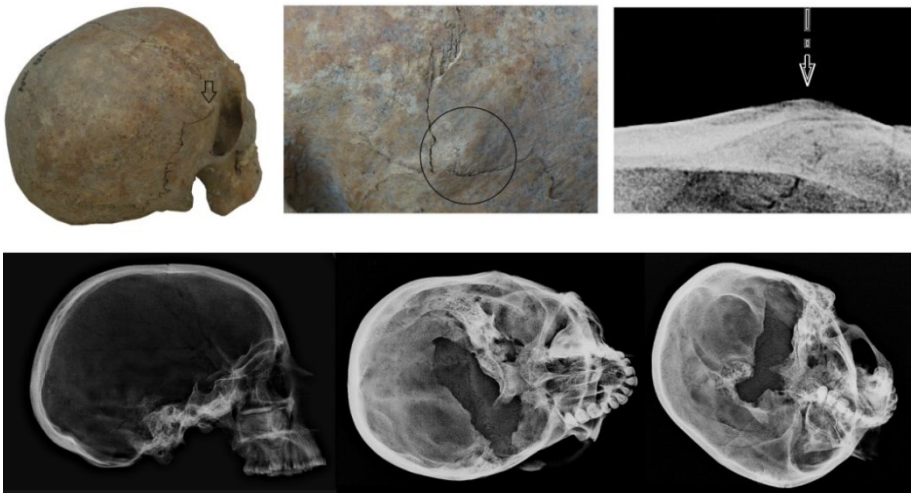

Figure 18 Neoplasm at the junction of the parietal and temporal bones.

Figure 19 Dental caries.

Figure 20 Enthesopathy of the iliac.

vertebral plates suggests the rudimental ankylosis (Figure 13a). The upper thoracic spine is involved in the complete fusion; both the bodies and the zygapophyseal joints of the 3th and the 4th thoracic vertebrae are fused. The vertebral bodies' fusion line is irregular, slight bumpy area is seen along it (Figure 13b), ankyloses of the facet joints present smooth appearance.

Cloacal openings are recognizable on the vertebral bodies (Figure 13). All of them are characterized with smooth margins, slight periosteal remodeling is recognizable around them. Resorption in the area of the diaphysis humerus (Figure 12), ankylosis (Figure 13a), cloacal openings on the vertebral bodies (рис. 13b), and these lesions are consistent with a diagnosis of tuberculosis (32). Tuberculosis it is a chronic infectious disease caused by one of the microorganisms of the group Mycobacterium. There is a direct human-human transmission caused by Mycobacterium tuberculosis, and there is transmission to humans from the consumption of bovine products caused by Mycobacterium bovis, and the latter transmission occurs relatively rarely (29, 33). The route of infection usually begins in the respiratory tract, leading to the formation of a primary focus in the lung and additionally to single or multiple foci in the regional hilar lymph nodes (33).

External auditory exostosis is observed on the skull (Figure 14a). External auditory exostosis is an abnormal broad-based projection of the temporal bone into the external auditory canal (34). They are usually rounded hyperostotic protrusions into the meatus that may partially or largely occlude the canal. Although benign and usually asymptomatic, it is an irreversible condition that can lead to potentially serious complications. Exposure to cold water and wind are recognised risk factors affecting external auditory exostosis prevalence and severity. Individual exhibits a circular blunt force trauma (15×9.8mm) in the left frontal bone with clear signs of healing; the innertable is intact. Button osteomas were identified in individual (Figure 14b). Button osteoma is a benign tumor that can be usually seen as a solitary circular, sharply demarcated bony nodule on the outer surface of the cranium. Its etiology is unknown but it has been suggested to be developmental, infectious or traumatic (35). It is seen on right parietal bone (Figure 14b). Symmetrical cuts made with a sharp object (symbolic trepanation) were found on the parietal bones of the individuals under study. It is accepted to name symbolical trepanations superficial (not through) manipulations where there is a slight break of the integrity of the arch of a skull (to injure a bone was accepted in certain specific places to create a certain geometrical pattern on an outer side of a brain capsule), fixed at carriers of various archaeological cultures. Trepanation not only mentioned integuments, but also extended in a periosteal top layer compact. As Lisowski (36) informs, the majority of cases of similar manipulation is fixed in females. Cradle deformationis also is revealed in individual.

Individual No 6.

The individual was identified as an infant aged 8-10 years. The skeleton is in a not complete of preservation (Figure 2). The front width of the lower jaw is 39.2 mm, the height of the symphysis is 25.4 mm. The shovel shape pronounced on the upper right mesially incisor. One can observe rotation of the right lower canine and moderately expressed marginal ridges on the lingual surface. Among the additional features, distal trigonid crest on the first molars are noted here.The enamel stain on the vestibular side of the lower molars is rated 6. Also a weak form of the linear enamel hypoplasia was detected on lower incisors and canine.

Perimortem trauma on this child on left innominate bone and on 1st lumbar vertebra. The proof for perimortem trauma on that individual is demonstrated in Figure 15. The left innominate bone of this individual exhibited a chop mark, which sprawling 11.3 mm in length, 1.5 mm in width, 6 (± 1)mm in depth. The cut surface is flat, sliced, indicating that the injury likely occurred around the time of death. The lumbar vertebra also demonstrated one chop stab from the forward portion, slightly to the left of center, and this trauma measured 10.9mm in length, 1.2 mm in width, 4 (± 1) mm in depth. Perimortem fractures show fracture patterning around injuries, such as concentric fractures, whereas postmortem fractures tend to lack such patterning and tend to shatter due to the dryness of the bone (17). Dry bone fractures tend to have more irregular edges while fractures of fresh bone tend to be clean and more linear with striations across the cut edges left by the weapon.

All spongy bone, including that of the vertebral bodies, is porous. In child we can see variety of TB, Pott's disease, which affects mainly the spinal column. These changes are caused by inflammatory process in vertebras.

Individual No 7.

The remains of individual 7 were buried in pythos (karas) (Figure 16). The skeleton belongs to a othirty to thirty nine years old female. The skull of the individual is characterized as dolichocranic (Table 1). It is absolutely low and relative tothe altitude-transverse index. The occiput is of large width. The external occipital protuberance is badly developed; andin the lateral norm the occiput is rounded. The mastoid is moderately developed. The forehead is of medium width. The frontal-transverse index is middle - mesozem. The glabella and superciliary arches are moderately developed. The face is tall, orthognathic; the nose is very narrow and very high, the orbits are of medium height and wide. The projection length of the lower jaw is large.The angles are deployed, the ramus mandible is medium. The tuberosity on the external surface of the angle and the internal surface of the angle is distinctly discerned on both sides. Fifteen of the forty-four studied discrete-varying markers are found in individual (foramina zygomaticofacialia, os zygomaticum bipartitum, spina processus frontalis ossis zugomatici /outgrowth/, stenocrotaphia /X-shaped/, processus temporalis ossis frontalis, os wormii suturae squamosum, foramina parietalia, foramina mastoidea, torus palatines (point 1), sutura palatina transversa /П-shaped/, sutura incisive, canalis craniopharyngeus, tuberculum praecondylare, foramina mentalia). We recorded superstructures those located where the superior oblique muscles insert (below the inferior nuchal line and lateral to the rectus capitis muscles) are known as retromastoid processes (RP) (Figure 17b). Morphogenesis and development of RP are the interactive outcome of a genetically underpinned, chronic activity induced multifactorial proceollows, chronic micro-trauma from arduous muscular overuse beginning at an early age (28). Cradle deformationis (Figure 17a) also is fixed on the skull.

The orbits show slight cribra orbitalia. Cribra orbitalia is associated with any number of diseases including scurvy, rickets, hemangiomas, and traumatic injuries; most of which are also associated with the root causes of malnutrition and chronic infectious diseases.

The female individual shows a paleopathological proof of a multiple osteomas condition. Skull has four neoformations: a) at the junction of the left parietal and temporal bones (dimensions 35 × 32.5 mm) (Figure 18), b) on the frontal bone (dimensions 4 × 4 mm), on the upper jaw in the region of the left third molar (dimensions 13.5 × 21.8 mm), the right third molar (dimensions 11 × 8.9 mm). The occurrence of multiple osteomas is a very rare condition. The literature examines different hypotheses with regard to their formation, including the idea that the lesions may be caused by congenital anomalies (37) or that chronic inflammation may originate within neoplastic proliferation (38). The development of osteomas may also be a consequence of trauma or embryogenetic changes. External auditory exostosis is observed on the skull.

The shape and the degree of attrition teeth correspond to the individual's age and labidodontic character of the bite. The mandibular right second and third molars were missing. The comparison of the mesiodistal and vestibulo-lingual dimensions of the mandibular molars revealed the following regularity. The vestibulo-lingual sizes (Table 2) of the first molars fall into the category of small values, third - average values. The mesio-distal sizes of the first molars fall into the category of average values. The crown height of the first molars is fall into the category of average values. There is no reduction of the crowns of the maxillary lateral incisors. The lingual and vestibular tubercles on the second premolars are approximately of the same size. The first maxillary molars are not reduced. On the second molars, the hypocone is strongly reduced (score 3+), and the metaconus is markedly reduced. The first mandibular molars havea5-tubercular structure with a "Y" crown-pattern. The third right molar is 6-tubercular with an "+" crown pattern. Dental caries is fixed on the upper right second premolar, first molar and lower left second molar (Figure 19). Dental caries is caused mainly by the organic acids, caused teeth tissue demineralization. Acids are mainly products of bacteria's fermentation (Streptococcus mutans and Lactobacills acidophilus).

The size of the ulnar and radial bone is on the low end of norm.The ulna and radius is also in all dimensions characterized by small values. The length of the femur (right) also characterized by small values. Poirer's facets located on the superolateral third of the femur at individual. The tibias are characterized by small values of the longitudinal dimensions. There is an additional articular area on the lower articular surface of the tibia. The present individual had a height of approximately 154.27cm.

Traces of physical exertion are observed on the bones of the upper and lower limbs. The crest of the lesser tubercle, the intertubercular sulcus of the humerus and the deltoid tuberosity of the

humerus are fairly well developed on the humeral bones. Suchlike development of the deltoid tuberosity of the humerus testifies to the strong development of the muscle of the same name which raises the upper limb up to a horizontal level and rotates the shoulder inward and outward. The radial roughness is well developed on the radial bones which are the reflection of the corresponding development of the muscles bending its shoulder and forearm. The quadrate pronator muscle is attached to the distal-lateral crest that is well developed on both ulnar bones. There is also a well developed lateral edge of the inferior limb of radius (both bones) to which this muscle is also attached. The presence of enthesitis in the iliac crest of both coxal bones is fixed at the individual. In both femora, the strong entheseal development and the articular traits of the hip joint suggest strong mechanical effort of the joint in extension and lateral stabilization and control of the thigh. Bony structures (tuberosity) revealed in dorsal to the auricular part of the sacroiliac joints (Figure 20). These changes are brought about by mechanical factors, such as the many years of horse-ridingetc, load on the femur, load on the pubic symphysis, etc. The strong development of the gluteal muscles and abductor muscles (mm. gluteus minimus and piriformis) indicate medio-lateral reinforcement to resist high mechanical stress on the proximal femoral shaft. The partial dislocation of the hip joint could be related to the medio-lateral mechanical effort needed to stabilize the trunk during erect posture and locomotion. The relief on the posterior surface of both tibias corresponding to the soleus line (third head of the triceps tibia muscle) is well developed.

Horseback riding is a possible skeletally influencing habitual activity for a woman, there is and other evidence for women participating in this activity (39). The archaeological material found with individual 5 did not suggest anything about her occupation or daily activities in life, but does suggest that she was of an elite status. The quality of the jewelry suggests that individual was well respected and likely of high social ranking. Horseback riding was an activity of the elite during the Iron Age. Individual was a horse rider, she have been socially significant in life and death.

This individual also suffered from degenerative joint disease, especially in the vertebral column (Figure 21). When severe trauma, strain or intervertebral disc degeneration occurs, the outer fibrous ring of the disc can tear. A herniation develops when the soft central portion of the disc is displaced beyond the interspace. The rider's posture causes the muscles in the back to contract to balance the spine and to prevent injury, which leads to large compressive forces being produced resulting in greater pressure placed on the intravertebral discs and facet joints (40).

Individual No 8.

The skeleton was poorly preserved and represented by only a fragmentary cranium, a mandible, and fragments of the postcranial skeleton. Dental development was consistent with an age at death at between 1.5 and 4.5 months old. This specimen exhibits abnormal porosity and the deposition of white new bone, mainly distributed bilaterally across bony projections (41) on the endocranial surfaces of the frontal bone. The skeleton shows excessive porosis and subperiosteal new bone formation (particularly on the humerus) (Figure 22c). The internal surface of the skull also reveals severe lesions (Figure 22b). Porous new bone forming a thick layer on top of the original bone surface can be detected over almost the entire endocranial surface of the frontal bone. These lesions may be indicative of haemorrhaging in the dural area and several clinical case studies have discussed the scorbutic aetiology of both extra, sub dural and sub arachnoid haemorrhage (42). On the upper parts of the frontal bones, the newly built bone formations are associated with abnormal, branching vessel impressions (Figure 22a). Scurvy, caused by vitamin C deficiency, leads to aberrant production of collagen, compromising the integrity of connective tissue and also manifests as frequent hemorrhages, particularly around alveoli and in areas surrounding entheses, where muscle contraction exerts pressureon the blood vessels. Although infants should receive a sufficient supply of vitamin C with breast milk, nutrient density in the breast milk can be extremely low in mothers with dietary deficiencies (43). Ortner and Ericksen (44) proposed a physiological relationship between scurvy and abnormal cortical porosity in several areas of the skull, including the maxilla, mandibular ramus, the greater wing of the sphenoid bone, and adjacent temporal squama, as well as on the orbital roof, all caused by chronic bleeding through weakened blood vessel walls. A list of other criteria that support a diagnosis of possible scurvy in juveniles, as compiled by Briekley and Ives (45) includes: new bone formation on the long bones, particularly towards the ends.

Figure 21 Violation integrity of the disk 5 of the thoracic vertebra.

Figure 22 Left zygomatic bone, fragments of the parietal and occipital bones with cribrotic changes on the surface of the skull (a), inflammatory processes in the form of periostitis (c) and white plaque on the endocranial of the left parietal bone (b).

Perimortem trauma on this child on left parietal, right innominate, and humerus bones. The proof for perimortem trauma on that individual is demonstrated in Figure 23. On the left parital bone, a trauma from an impact with a blunt object was revealed (dimensions 4.3×3.7×4.7mm) (Figure 23a). The trauma was received perimortem the individual's death. On a fragment of the right iliac bone was trauma from an impact with a sharp object was revealed (length 4.9 mm, width 4.8 mm) (Figure 23c). On the right humerus was another trauma from an impact with a sharp object was revealed (dimensions 6×5×3.5mm) (Figure 23b).

Individual No 9.

The individual was identified as an infant aged 5-6 years. The skull was poorly preserved and represented by only a fragmentary. The skeleton shows excessive porosis formation, periosteal reaction (particularly in the lower extremities of the femur (Figure 24a), the tibia and fibula).The morphological pattern appears to be typical for local ossified hemorrhages (i.e. hemorrhages that continued for a certain time). Radiographs of long bone diaphyses show evenly spaced growth arrest lines (Harris lines). Harris lines (46) are transverse scleroticlayers in the metaphysial parts of long bones, reflecting the episodes of delayed orarrested development of the

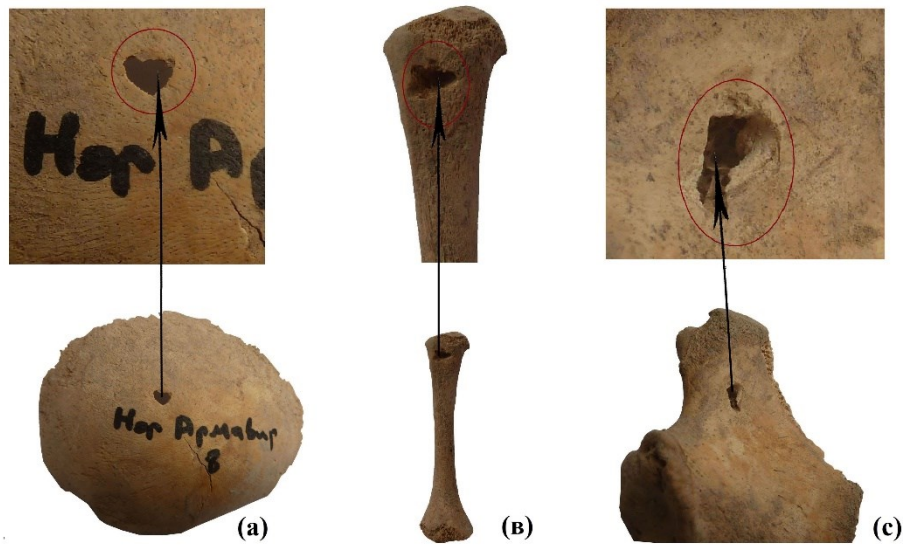

Figure 23 Stab wounds on the parietal, innominate and humerus bones.

Figure 24 Cribrotic changes on the surface of the femur, diaphysic growth retardation line. Note the cortical porosity and honeycomb appearance of metaphyseal trabeculae.

longitudinal growth of the bone (Figure 24b). Harris lines may be formed only in the period of the longitudinal growth of bones.

Individual No 10.

The skeleton was poorly preserved and represented by only fragments of the postcranial skeleton. Sex cannot be unambiguously determined, biological age refers to the adultus category. The size of the right ulnar and radial bones characterized small length. The radial roughness is moderately (not weakly), the quadrate pronator muscle is attached to the distal-lateral crest that is moderately developed on ulnar bone. The present individual had a height of approximately 161 cm (Table 3).

Conclusion

This article the results of analysis of human burials from the Nor Armavir site, in Armenia. The material of the study was the skeletal remains of 10 individuals (one man, three women, 5 children and one without sex definition) discovered in August 2019 during excavations of New Armavir grave. For the first time, a comprehensive paleoanthropological analysis of the data was obtained for this grave. Five of the three individuals who were able to measure both skull diameters (1,8) were dolichocraned, and two of them were mesocraned. One skull (№3) has an average height diameter (ba–br), the other one is very small (№7) and the third is large (№5) . The width of the back of the head of the two is medium (№2, 5) and the width of the two is large (№3, 7). The facial skeleton is characterized by medium

(№3) and large (№7) width, with one skull (№3) having a small face height , the other at the boundary between medium and large magnitudes (№5) , and the third being large (№7) . The width of orbits (от mf) is characterized by very large values (№3, 5, 7), the height of two is medium (№5, 7), one is very large (№3). The height of the nose varies from medium (№3) to very large values (№5, 7), the width from very small (№5, 7) to medium dimensions (№3). The simotic and dacrial pointers are large. Two craniological complexes can be conditionally isolated as part of this group. The first is of the low-head mesocrane type, the second high-head dolichocrane type. The distribution of certain genetically deterministic (non metric traits) features allows for certain related relationships between individuals. At six individuals are found foramina zygomaticofacialia, os wormii suturae squamosum, foramina parietalia, at five - processus temporalis ossis frontalis, foramina mastoidea, sutura incisiva, at four – os zygomaticum bipartitum tripartitum, os wormii suturae lambdoidea, форма sutura palatina transversa (П-shaped), canalis craniopharyngeus, at three - canalis condyloideus, foramina mentalia, форма stenocrotaphia (X-shaped), at two - spina processus frontalis ossis zugomatici (straight) и (protruding), foramina mastoidea (at the seam), torus palatines (point 1), torus palatines (point 1), lack of foramina spinosum, tuberculum praecondylare. The odontological complex is of the southern graceful type with a high level of reduction of the hypoconus of the second upper molars, small tooth sizes. At the individual level, the total size and shape of the body of the adult population has been analysed. Labour burdens are recorded in both women and men. The tradition of inadvertently changing the shape of the head in a given sample probably caused a specific way of caring for the infant in the early years of his life and a long stay in a certain cradle. Traces of pathological processes on skeletons have been revealed and their etiology has been reconstructed. The structure of the paleopathological profile of the sample is dominated by inflammatory diseases, abnormalities and injuries. It has been established that the state of health of individuals buried in the grave was unsatisfactory, as evidenced by the large number of pathologies. The poor sanitation in Armavir resulted in sporadic outbreaks of various infectious diseases (such tuberculosis, periapical lesion, etc.). The hypothesis is that such living conditions resulted in relatively poor health, especially in children, which should reflect in increased frequency of skeletal and dental indicators of subadult stress and indicators of non-specific infectious diseases. In our study, 3 out of 4 children skeletons with evident lesions, that were defined as diagnostic of scurvy. An anthropological analysis of 10 skeletons revealed at the 4 individuals penetrating wounds on the skeletons. Although considerable uncertainty remains, we believe that the most likely conclusion is that Nor Armavir burials represent a place for at least some sacrificed individuals dedicated as offerings. Something ritualistic clearly did occur with these remains.

This initial analysis is only the starting-point for reconstructing information about the community who were buried at Nor Armavir burials. At later stages of the research vital information from secondary sources will be analysed, and will combine a variety of scientific investigations in an attempt to glean as much information as is possible about the Armavir population in 7c. BC.

References

1. Khorenatsi M. History of Armenia. New translation N.O. Emin (with attachments and attachments). Posthumous publication. Moscow, 1893 (In Rus.).
2. Hmayakyan S., Tiratsyan N., Hmayakyan M. Pithos and clay-cist burials excavated in Argishtikhinili, 2016: preliminary report. In Beyond Aragats. Archaeological Studies in Memory of Telemak Khachatryan: Avetisyan et al. Yerevan, pp. 175-181, 2018 (In Armenian)
3. Acsádi Gy., Nemeskéri J. History of human life span and mor¬ti¬laty. Budapest, 1970.
4. Buikstra J.E., Ubelaker D.H. Standards of data collection from human skeletal remains. Arkansas Archaeol. Survey Research Series. 44. Fayetteville, 1994.
5. Phenice TW. A newly developed visual method of sexing the os pubis. Am J Phys Anthropol. 1969; 30:297-302
6. Meindl RS, Lovejoy CO, Mensforth RP, Carlos LD. Accuracy and direction of error in the sexing of the skeleton: Implications for paleodemography. Am J Phys Anthropol. 1985; 68:79-85.
7. Lovejoy CO, Meindl RS, Pryzbeck TR, Mensforth RP. Chronological metamorphosis of the auricular surface of the ilium: A new method for the determination of adult skeletal age at death. Am J Phys Anthropol. Am J Phys Anthropol. 1985; 68:15-28.

8. Gilbert BM, McKern TW. A method for aging the female os pubis. Am J Phys Anthropol. 1973; 38:31-38.
9. Katz D, Suchey JM. Age determination of the male os pubis. Am J Phys Anthropol. 1986; 69:427-435.
10. AlQahtani SJ, Hector MP, Liversidge HM. Brief Communication: The London Atlas of Human Tooth Development and Eruption. Am J Phys Anthropol. 2010; 42(3): 481-490.
11. Movsesyan AA, Mamonova NN, Richkov YuG. The program and method of research of anomalies of a skull. Anthropology questions. 1975; 51: 127-150.
12. Zubov AA. Odontology: A Method of Anthropological Research. Moscow: Science, 1968.
13. Zubov AA. Ethnic odontology. Moscow: Science, 1973.
14. Alekseev VP, Debets GF. Kraniometriya (metodika antropologicheskih issledovanij) [Craniometry (methods of anthropological research)]. Moscow: Science, 1964.
15. Haeussler A, TurnerCG,. The dentition of Central Asia and the quest for New World ancestors. Special Issue 2. In Culture, Ecology, and DentalAnthropology: Lukacs JR. J Hum Evol.1992; 273–297.
16. Khudaverdyan A.Yu. Illuminating the processes of microevolution: A bio¬archaeological analysis of dental non-metric traits from Armenian Highland. HOMO - Journal of Comparative Human Biology. 2018; 69: 304–323.
17. Roberts C, Manchester K. The archaeology of disease (3rd ed.). Ithaca: Cornell University Press, 2005.
18. Trotter M, Gleser G. A Re-evaluation of Estimation of Stature Based on Measurements of Stature Taken During Life and of Long Bones after Death. Am J Phys Anthropol. 1958; 16: 79-123
19. Alekseev VP. Osteometriya (metodika anthropologicheskikh issledovanij) [Osteometry (methods of anthropological research)]. Moscow: Science, 1966.
20. Caffey J. The Whiplash Shaken Infant Syndrome: manual shaking by the extremities with whiplash-induced intracranial and intraocular bleedings, linked with residual permanent brain damage and mental retardation. Pediatrics. 1974; 54: 396–403
21. Kempe CH, Silverman FN, Steele BF, Droegemueller W, Silver HK. The battered-child syndrome. Child Abuse and Neglect. 1985; 9: 143–154.
22. Lovell NC. Trauma analysis in paleopathology. Yearbook J Phys Anthropol. 1997; 40:139-170.
23. Adams JC, Hamblen D. Outline of Fractures, Including Joint Injuries. New York: Churchill Livingstone, 1999.
24. Teh J, Firth M, Sharma A, Wilson A, Reznek R, Chan O. Jumpers and Fallers: A Comparison of the Distribution of Skeletal Injury. Clinical Radiology. 2003; 58:482-486.
25. Capasso L, Kennedy K, Wilczak C. Atlas of occupational markers on human remains. Teramo: Edigrafital S.P.A. 1999.
26. Angel JL. The reaction area of the femoral neck. Clinical Orthopaedics. 1964; 32:130-142.
27. Khudaverdyan AYu. Artificial Deformation of Skulls from Bronze Age and Iron Age Armenia. The Mankind Quarterly. 2016; 56 (4): 513-534.
28. Khudaverdyan AYu. Tumpline Deformation on Skulls from Late Bronze and Early Iron Age Armenia: A Cause of Enigmatic Cranial Superstructures? The Mankind Quarterly. 2018; 5 (4): 8-30.
29. Aufderheide AC, Rodríguez-Martín C. The Cambridge encyclopaedia of human palaeopathology. Cambridge: Cambridge University Press. 1998.
30. Scott EC. Dental Wear Scoring Technique. Am J Phys Anthropol. 1979; 51: 213-217.
31. Goodman A.H., Rose J.C. Assessment of systemic physiological perturbations from dental enamel hypoplasias and associated histological structures. Yearbook J Phys Anthropol. 1990; 33: 59–110.
32. Hershkovitz I, Greenwald CM, Latimer B, Jellema LM, Wish-Baratz S, Eshed V, Dutour O, Rothschild BM. Serpens endocrania symmetrica (SES): a new term and possible clue for identifying intrathoracic disease in skeletal populations. Am J Phys Anthropol. 2002; 118: 201–216
33. Ortner DJ. Identification of Pathological Conditions in Human Skeletal Remains. Academic Press, 2003.
34. Mariezkurrena A, Gómez Suárez J, Luqui Albisua I, Vea Orte JC, Algaba Guimerá J. Prevalence of exostoses surfers of the Basque coast. Acta Otorrinolaringológica Española. 2004; 55: 364–368.
35. Eshed V, Latimer B, Greenwald CM, Jellema LM, Rothschild BM, Wish-Baratz S, Hershkovitz I. Button Osteoma: Its Etiology and Pathophysiology. Am J Phys Anthropol. 2002; 118:217–30.
36. Lisowsky FP. Prehistoric and early Historic Trepanation. In Diseases in Antiquity: Brothwell D, Sandison A. Thomas Publication, Springfield, pp. 651–672, 1967.
37. Wijn MA, Keller JJ, Giardinello FM, Brand HS. Oral and maxillofacial manifestations of familial adenomatous polyposis. Oral Diseases. 2007; 13: 360.
38. Sahin A, Yildirim N, Cingi E, Atasoy MA. Frontoethmoid sinus osteoma as a cause of subperiosteal orbital abscess. Advances in Therapy. 2007; 24: 571-4.
39. Khudaverdyan AY, Yengibaryan AA, Hobosyan SG, Hovhanesyan AA, Saratikyan AA. An Early

Armenian female warrior of the 8–6 century BC from Bover I site (Armenia). Int J Osteoarchaeol. 2020; 30: 119–128.
40. Nicol G, Arnold GP, Wang W, Abboud RJ. Dynamic pressure effect on horseand horse rider during riding, Sports Engineering. 2014; 17(3):143-150
41. Lewis ME. Endocranial lesions in non-adult skeletons: understanding their aetiology. Int. J. Osteoarchaeol. 2004; 14, 82–97.
42. Ahuja SR, Karande S. An unusual presentation of scurvy following head injury. Indian Journal of Medical Sciences. 2002; 56 (9): 440-442
43. Morseth, M.S., Torheim, L.E., Chandyo, R.K., Ulak, M., Shrestha, S.K., Shrestha, B., Pripp, A.H., Henjum, S., 2018. Severely inadequate micronutrient intake among children 9-24 months in Nepal-The MAL-ED birth cohort study. Matern. Child Nutr. 14 (2), e12552.
44. Ortner DJ, Ericksen MF. Bone changes in the human skull probably resulting from scurvy in infancy and childhood. Int. J. Osteoarchaeol. 1997; 7: 212–220.
45. Briekley M, Ives R. The Bioarchaeology of Metabolic Bone Disease. Academic Press. 2008.
46. Harris H. Bone growth in health and disease. Oxford Medical Publications. London: Oxford University Press, 1933.

Table 1 Individual, average sizes and indexes of skulls from Nor Armavir.

		I 4-6	II ♀ 20-29	III ♂ 60+	IV 8-10	V ♀ 50-59	VII ♀ 30-39
1	Maximum cranial length (g-op)	164	-	195	171	184	180
8	Maximum cranial breadth (eu-eu)	116	137	136	130	141	135
8:1	Cranial index	70.8	-	69.8	76.1	76.64	75.0
17	Height diameter (ba)	-	-	135	127	132.5	118
17:1	Height-length index	-	-	69.3	74.3	72.02	65.6
17:8	Height- breadth index	-	-	99.3	97.7	93.98	87.5
20	Height diameter (po)	-	-	123	117	122	107.5
20:1	Height-length index	-	-	63.1	68.5	66.31	59.8
20:8	Height- breadth index	-	-	90.5	90.0	86.53	79.7
9	Minimum frontal breadth (ft-ft)	78.8	-	103	89.8	101.8	95
9:8	Frontal - breadth index	67.94	-	75.8	69.1	72.2	70.4
10	Maximal frontal breadth	93	-	118	111	116?	118
11	Cranial base width	95	-	124	102.5	118.3?	125
12	Occipital breadth	97	107	115	102	106	111
45	Bizygomatic breadth (zy-zy)	94	-	136	106?	-	128
48	Upper facial height	45	-	65.7	84	68.5	70,5
48:45	Upper facial index	47.9	-	48.4	79.3	-	55.1
55	Nasal height (n-ns)	35.2	-	51	41	51.8	55
54	Nasal breadth (al-al)	20	-	25.5	19.9	21	22.6
54:55	Nasal index	56.9	-	50.0	48.6	40.6	41.1
51	Orbital breadth (d-ec)	33.2	-	46.3	37.8	44	43
51a	Orbital breadth (ect-d)	29.8	-	42.8	33	38.5	40
52	Orbital height bicondylar width	30.5	-	37	32	34	35
52:51	Orbital index (mf)	91.9	-	79.92	84.7	77.3	81.4
52:51	Orbital index (d)	102.4	-	86.5	96.97	88.4	87.6
DC	Dacryal chord	-	-	24.2	19	20.5	22
DS	Dacryal subtense	-	-	11	9.5	13.8	13
DS:DC	Dacryal index	-	-	45.5	50.0	67.4	59.1
SC	Simotic chord	-	-	9.9	9	7.7	8.8
SS	Simotic subtense	-	-	6	3.5	7	4.2

SS:SC	Simotic index	-	-	60.7	38.9	90.91	47.8
32	Frontal pronfile angle (n-m)	-	-	87	-	80	79
	Frontal pronfile angle (g-m)	-	-	84	-	78	75
72	Total facial angle	-	-	87	-	85	81
73	Mid-facial angle	-	-	88	-	84	82
74	Alveolar angle	-	-	92?	-	89	88
75(1)	Nasal protrusion angle	-	-	27	-	38?	34
77	Naso-malar angle (fmo-n-fmo)	-	-	131	-	133	136
<zm	Zigo-maxillary angle (zm`-ss-zm`)	-	-	126	-	126	126

Table 2 Individual sizes of teeth from the Nor Armavir monument.

	Ind. II	**Ind. IV**	**Ind. VI**	**Ind. VII**	**Ind. II**	**Ind. II**	**Ind. VI**	**Ind. VII**
	Maxilla				Mandible			
	VLcor							
	right/ left	right/ left	right/ left	right/ left	right/ left	right/ left	right/ left	right/ left
I1	-/-	-/-	6.2/6.1	6.2/6.2	-/-	-/-	7.1/-	7/7
I2	-/-	-/-	6.3/6.2	6.3/6.5	-/-	6.8/6.3	-/-	6.8/6.7
C	-/-	-/-	7.8/7.7	7.5/7.3	-/-	-/-	-/-	8.3/8
P1	-/-	7.9/7.9	7.8/7.8	7.3/7.5	-/8.6	-/-	-/-	8.6/8.8
P2	-/-	-/-	-/-	8.2/7.8	8.3/-	9.3/-	-/-	-/9.2
M1	-/10.8	-/-	9.9/-	9.8/10.4	10.1/10.8	10.2/10.4	-/-	10.8/11.2
M2	9.2/8.9	9.8/-	-/-	-/-	10.4/10.3	10.8/-	-/-	10.5/-
M3	10.5/9.3	-/-	-/-	-/9.9	11/11.2	-/-	-/-	10.7/-
	MDcor							
I1	-/-	-/-	6/6	6/5.8	-/-	-/-	9.1/-	7.3/7.5
I2	-/-	-/-	6.5/6.5	6.3/6.2	-/-	7.1/7	-/-	6.6/6.8
C	-/-	-/-	6.8/6.8	7/6.9	-/-	-/-	-/-	7/8
P1	-/-	7.3/7.5	7/7	7.2/7.2	-/7	-/-	-/-	7/7
P2	-/-	-/-	-/-	7/7	6.8/7	6.7/-	-/-	6/6.6
M1	-/11	-/-	-/-	11/11.6	10.8/11	10/10	-/-	11.6/11.1
M2	9.7/9.2	10.8/-	-/-	-/-	8.2/9	9.8/-	-/-	9/-
M3	10.8/11	-/-	-/-	-/11.1	10.3/9.8	-/-	-/-	9.1/-
	Hcor							
M1	-/5.3	-/-	7.5/-	5.2/5.8	7/6.8	6.8/6.5	-/-	5.8/5.2
M2	7/6.5	7.2/-	-/-	-/-	7.6/-	6.5/-	-/-	6.2/-
M3	-/7	-/-	-/-	-/7	6/7.8	-/-	-/-	5.8/-
	MDcol							
M1	-/8.7	-/-	7.8/-	9.3/9.1	7.2/7.7	7.8/8.3	-/-	7.6/7.7
M2	8.9/8.3	8.6/-	-/-	-/8.8?	6.8/7	7.2/-	-/-	6.5/-
M3	9.2/10	-/-	-/-	-/9.1	7.3/7.5	-/-	-/-	6.7/-
	MD × VL							
M1	-/118.8	-/-	-/-	107.8/120.64	109.08/118.8	102/104	-/-	125.3/124.4
M2	89.24/81.88	105.84/-	-/-	-/-	85.28/92.7	105.9/-	-/-	94.5/-
M3	113.4/102.3	-/-	-/-	-/109.89	113.3/109.76	-/-	-/-	97.4/-
	Icor (VL / MD) × 100							
M1	-/98.19	-/-	-/-	89.1/89.66	93.6/98.2	102/104	-/-	93.2/100.91
M2	94.85/96.74	90.7/-	-/-	-/-	126.9/114.5	110.3/-	-/-	116.7/-
M3	97.23/84.55	-/-	-/-	-/89.19	106.8/114.3	-/-	-/-	117.6/-
	Mcor MD + VL / 2							
M1	-/10.9	-/-	-/-	10.4/11	10.5/10.9	10.1/10.2	-/-	11.2/11.2
M2	9.45/9.05	10.3/-	-/-	-/-	9.3/10.5	10.3/-	-/-	9.8/-
M3	10.65/10.15	-/-	-/-	-/10.5	10.7/10.5	-/-	-/-	9.9/-

Table 3 Individual sizes and indexes of skeleton bones from the Nor Armavir monument.

Feature	Individual II		Individual III		Individual V		Individual VII		Individual X	
	right	left	right	left	right	left	right	left	right	left
	Humerus									
1. Maximal length	-	301	324	320	317.8	-	-	-	-	-
2. Total length	-	298	322	316	314.7	-	-	-	-	-
3. Upper epiphysis breadth	-	43	51	49	45.2	44.5	-	-	-	-
4. Lower epiphyseal width	-	52.3	62.2	61.5	-	54.3	-	56.5	-	-
5.Maximal midshaft breadth	-	21	23.7	22.6	21.7	20.3	-	23	-	-
6. Minimal midshaft breadth	-	16	18.6	18	16	16.2	-	17	-	-
7. Minimal shaft circumference	-	54.5	62	62	56	55	-	57	-	-
7a. Midshaft circumference	-	61	70	69	63	62	-	66	-	-
7:1 Robusticity index	-	18.2	19.2	19.4	17.7	-	-	-	-	-
6:5 Cross-section index	-	76.2	78.5	79.7	73.8	79.9	-	73.92	-	-
	Radius									
1. Maximal length	-	-	-	-	-	243	223	219	215	-
2. Physiological length	235	-	-	-	-	231	215	210	207	-
4.Cross-section diameter	14.8	14.2	-	-	-	15.2	15.2	12.3	14	-
5. Sagittal shaft diameter	11	10.9	-	-	-	11	11.5	11	9.5	-
3. Minimal shaft circumference	39	40	-	-	-	39	39	38	36	-
3:2 Robusticity index	16.6	-	-	-	-	16.9	18.2	18.1	17.4	-
5:4 Cross-section index	74.4	76.8	-	-	-	72.4	75.7	89.5	67.9	-
	Ulna									
1. Maximal length	-	-	272	-	-	254	243	237	238	-
2. Physiological length	-	-	235	-	-	227	215	211	207	-
11. Sagittal diameter	-	-	14.4	14.2	-	12	10	8.9	10.6	-
12. Transverse diameter	-	-	17	19.2	-	15.6	19.8	11	15.8	-
13. Upper transverse diameter	21	21	20	-	-	19.9	22.8	21.2	18.3	-
14. Upper sagittal diameter	24	22	25	-	-	24	24.8	22.3	23.2	-
3. Minimal shaft circumference	-	-	36	37	-	43	37	35	31	-
3:2 Robusticity index	-	-	15.4	-	-	18.95	17.6	16.6	14.98	-
11:12 Cross-section index	-	-	84.8	73.96	-	76,93	50,6	80,91	67.1	-
13:14 Platyleny index	87,5	-	80.0	-	-	82.92	91.94	95.1	78.9	-
	Femur									
1. Maximal length	409	-	440	451	-	-	427	417	-	-
2. Natural length	398	-	436	444	-	-	417	409	-	-
21. Condylar breadth	65.8	-	79	79.9	-	-	73	72.2	-	-
6. Sagittal diameter of midshaft	26	25.2	31.3	31.1	-	-	27	25.2	-	-
7. Transverse midshaft diameter	26.3	26	27	27.8	-	-	25.8	26	-	-
9. Upper transverse shaft diameter	31.2	32	30	29.8	-	-	33	33	-	-
10. Upper sagittal shaft diametere	23	23.4	27	25.6	-	-	23.5	23.2	-	-
8. Midshaft circumference	79	81	89	92	-	-	81	80	-	-
8:2 Robusticity index	19.9	-	20.5	20.8	-	-	19.5	19.6	-	-
6:7 Pilastry index	98.9	96.93	115.93	111.9	-	-	104.7	96.93	-	-
10:9 Platymery index	73.8	73.2	90	85.91	-	-	71.3	70.4	-	-
	Tibia									
1.Full length	346	-	357	-	-	-	340	339	-	-
2. Condylo-talar length	303.5?	-	304.5	304	-	-	302.5	302.5	-	-
1a. Maximal length	349	-	363	-	-	-	342	342	-	-
5. Upper epiphysis breadth	-	65	78.6	76	-	-	68	71	-	-
6. Lower epiphysis breadth	38	-	47	45?	-	-	42.8	41.5	-	-

8. Sagittal diameter at midshaft level	26.5	26	32	32.8	-	-	25	23	-	-
8a. Sagittal diameter at the nutrient foramen level	32	31,5	37	35	-	-	33.8	27	-	-
9. Transverse diameter at midshaft level	19.3	20.1	21	21.2	-	-	19.7	19	-	-
9a. Transverse diameter at the nutrient foramen level	21.1	21.8	24	23	-	-	24	19.8	-	-
10. Midshaft circumference	74	75	82	82	-	-	72	72	-	-
10b. Minimal shaft circumference	67	-	75	76	-	-	66.5	66	-	-
9:8 Cross-section index	72.9	77.4	65.7	64.7	-	-	78.8	82.7	-	-
10b:1 Robusticity index	19.4	-	21.1	-	-	-	19.6	19.5	-	-
9a:8a Cross-section index	65.94	69.3	64.9	65.8	-	-	71.1	73.4	-	-
10:1 Robusticity index	21.4	-	22.97	-	-	-	21.2	21.3	-	-
	Fibula									
1. Full length	-	-	-	-	-	-	332.5	-	-	-
	Skeletal proportions									
R1:H1 Brachial index	-	-	-	-	-	-	-	-	-	-
T1: F2 Tibio-femoral index	86.94	-	81.9	-	-	-	81.6	82.9	-	-
H1+R1/F1+T1 Intermembral index	-	-	-	-	-	-	-	-	-	-
H1+R1/ F2+T1 Intermembral index	-	-	-	-	-	-	-	-	-	-
H1:F2 Humero-femoral index	-	-	74.4	72.1	-	-	-	-	-	-
R1:T1 Radio-tibial index	-	-	-	-	-	-	65.6	64.7	-	-
Body length (average)	152.4		165.03		159.6		154.27		161.76	

Table 4 Point characteristic of the development of the relief of long bones.

	Individual II		**Individual III**		**Individual V**	
	right	left	right	left	right	left
Humerus						
Crista tuberculi minoris, crista tuberculi majoris	-	2	3	2.5	2	2
Tuberositas deltoidea	-	1.5	2,5	2,5	1	2
Tuberculum majus, tuberculum minus	-	2.5	2,5	3	1,5	2
Margi lateralis, medialis et anterior Epicondili lateralis et medialis	-	1.5	2.5	2.5	1	1
In total	-	1.9	2.63	2.63	1.38	1.75
Radius						
Tuberositas radii	2.5	2	-	-	-	3
Margo unterossea	2	2	2.5	-	-	2
Furrows for extensor tendons	2	2	-	-	2.5	2.5
Processus styloideus	-	2	-	-	2	3
In total	2.17	2	-	-	2.25	2.63
Ulna						
Margo interossea, margo posterior	2	2	3	3	-	2.5
Crista musculi supinatoris	1.5	2	2	-	-	1
Tuberositas ulnae	1.5	2	2.5	-	-	2
In total	1.67	2	2.5	3	-	1.,84
Femur						
Trochanter major	1.5	1.5	1.5	2	-	-
Trochanter minor	2		2	2.5	-	-
Tuberositas glutea	2	2	2.5	2.5	-	-
Linea aspera	2.5	2	2.5	3	-	-
Epicondili	1.5		2	2	-	-
In total					-	-

Tibia						
Tuberositas tibiae	1.5	1.5	2	2	-	-
Margo anterior, margo interossea	2	2	2.5	2	-	-
Linea m. solei, m. soleus	1	1	2.5	2	-	-
Furrows for extensor tendons	1		3	2?	-	-
In total					-	-
Fibula						
The edges development	2	2	3	3	2.5	2.5

Table 4 (continued).

	Individual VII right left		**Individual X** right left	
Humerus				
Crista tuberculi minoris, crista tuberculi majoris	-	-	-	-
Tuberositas deltoidea	-	2.5	-	-
Tuberculum majus, tuberculum minus	-	-	-	-
Margi lateralis, medialis et anterior Epicondili lateralis et medialis	-	2	-	-
In total	-	2.25	-	-
Radius				
Tuberositas radii	2	2	1.5	-
Margo unterossea	2.5	3	2	-
Furrows for extensor tendons	2.5	2.5	2	-
Processus styloideus	2.5	2.5	2	-
In total	2.38	2.5	1.88	-
Ulna				
Margo interossea, margo posterior	3	3	2	-
Crista musculi supinatoris	2	1.5	1	-
Tuberositas ulnae	2.5	2	1	-
In total	2.5	2.17	1.34	-
Femur				
Trochanter major	2	2	-	-
Trochanter minor	2	2	-	-
Tuberositas glutea	2	2	-	-
Linea aspera	2.5	2.5	-	-
Epicondili	2	2	-	-
In total	2.1	2.1	-	-
Tibia				
Tuberositas tibiae	1.5	1.5	-	-
Margo anterior, margo interossea	2	2	-	-
Linea m. solei, m. soleus	2	2	-	-
Furrows for extensor tendons	2	2	-	-
In total	1.88	1.88	-	-
Fibula				
The edges development	3	3	-	-